

Supporting information

A high-rate cathode material hybridized by in-site grown Ni-Fe layered double hydroxide and carbon black nanoparticles

Shuzhen Chen,^a Min Mao,^a Xi Liu,^a Shiyu Hong,^a Zhouguang Lu,^b Shangbin Sang,^a Kaiyu Liu,^a Hongtao Liu^{a*}

^aCollege of Chemistry and Chemical Engineering, Central South University, Changsha 410083, China

^bDepartment of Materials Science and Engineering, South University of Science and Technology of China, Shenzhen 518055, China

* Corresponding author. E-mail: liuht@csu.edu.cn; Tel: +86 731 8887 9616

XRD

To probe the as-obtained Ni-Fe LDHs and the hybrid HT-LDH/CB material, we have carried out XRD patterns. As is shown in Figure S1, Ni-Fe LDHs exhibits the typical characteristics of LDH materials. The characteristic bands at $2\theta = 9.9^\circ$, 22.8° , 34.5° and 60.3° , corresponding to the (003), (006), (101+012) and (110+113) diffraction peaks, respectively, are in good agreement with those of standard patterns of $\text{Ni}_6\text{Fe}_2(\text{SO}_4)(\text{OH})_{16}\cdot 4\text{H}_2\text{O}$ (JCPDS no.:42-0573). By the way, the atomic rate of Ni and Fe (3:1) can also be proved by XPS test. From these parameters, the basal spacing of Ni-Fe LDHs is estimated to 0.78 nm, which is in good agreement with that reported for Ni-Fe LDHs in the previous literature.^{1, 2} HT-LDH/CB hybrid displays similar characteristic bands to Ni-Fe LDHs while the (003) diffraction peak is more sharp and skewing to the right. This indicates the HT-LDH/CB hybrid owns better crystalline forms. Additionally, no residual peaks have been observed, confirming the absence of contaminant phases.

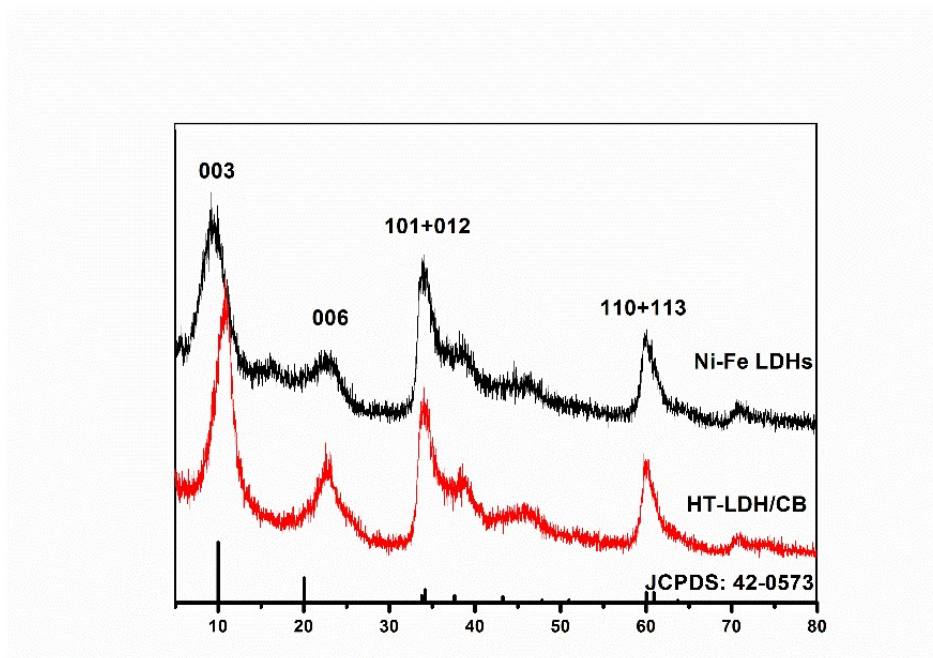


Figure S1 XRD patterns of Ni-Fe LDHs and HT-LDH/CB

XPS

XPS is a reliable method for investigating the oxidation state of atoms in the top few layers of material surfaces with partially filled valence bonds. Figure S2 shows the XPS survey spectra of Ni-Fe LDHs and HT-LDH/CB. Figure S3 indicates the core-level XPS spectra of S, O, C of Ni-Fe LDHs and HT-LDH/CB. The S 1s peaks at 168.2 eV is hexavalent sulfur elemental typically, which is consistent with those of standard patterns of $\text{Ni}_6\text{Fe}_2(\text{SO}_4)(\text{OH})_{16}\cdot 4\text{H}_2\text{O}$.³

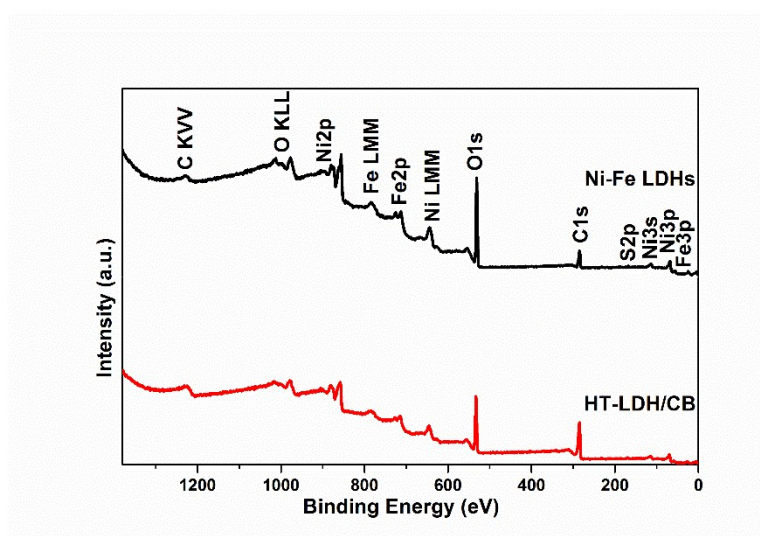


Figure S2 Survey XPS spectra of Ni-Fe LDHs and HT-LDH/CB

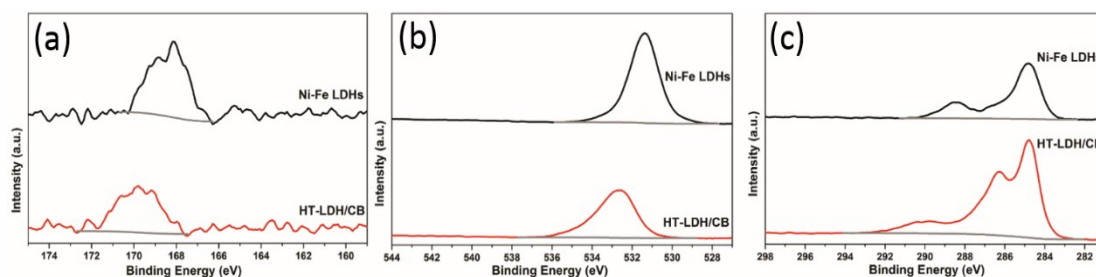


Figure S3 Core-level XPS spectra of Ni-Fe LDHs and HT-LDH/CB (a, S 2p; b, O 1s; c, C 1s)

FTIR

The FT-IR spectrum of Ni-Fe LDHs and the hybrid HT-LDH/CB material in the region between 400 and 4000 cm^{-1} are shown in Figure S4. The infrared bands around 3443 cm^{-1} can be ascribed to the OH-stretching vibration in the brucite-like layers and interlayer water, and the strong absorption at 1622 cm^{-1} is attributed to the hydroxyl deformation mode of the interlayer water molecules. They support the ideas that the sample has OH groups and that water molecules are present in the interlayers. The mode located at about 1106 cm^{-1} is assigned to S=O stretching vibration. The band observed at 665 cm^{-1} attributed to Fe-O or Ni-O. These results are in good agreement with the XRD data.^{2,4}

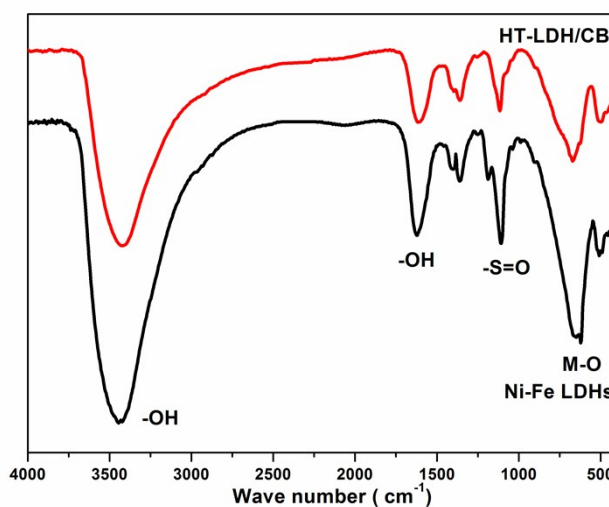


Figure S4 FT-IR spectra of Ni-Fe LDHs and HT-LDH/CB

CV

Shown in Figure S5 are the CV curves of Ni-Fe LDHs, HT-LDH/CB and PM-LDH/CB at scan rates 5~50 $\text{mV}\cdot\text{s}^{-1}$. The peak current increases with the scan rate, and the peak area of the HT-LDH/CB electrode is apparently larger than that of the Ni-Fe LDHs or PM-LDH/CB electrode, implying a higher utilization of active material and larger electrode capacity of the HT-LDH/CB electrode.

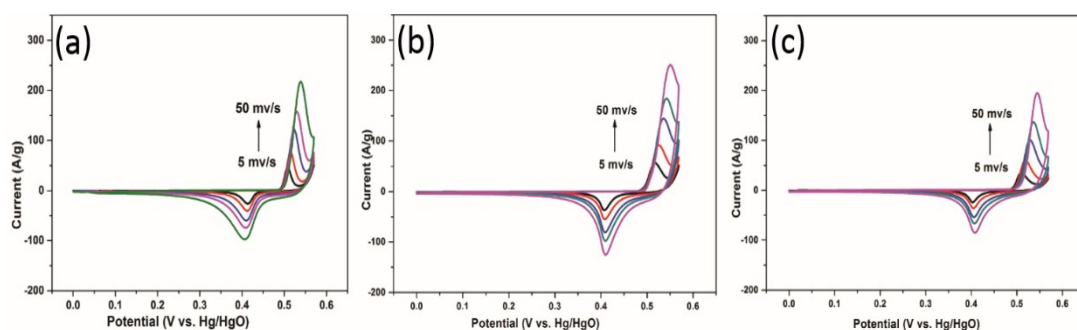


Figure S5 CV curves of (a, Ni-Fe LDHs; b, HT-LDH/CB; c, PM-LDH/CB) at different scan rates of 5, 10, 20 and 50 $\text{mV}\cdot\text{s}^{-1}$ in 6.0 M KOH solution

Table S1 XPS patterns of the Ni-Fe LDH product

Name	Start BE	Centre BE	End BE	Height CPS	FWHM eV	PP Height CPS	PP At. %	Title Scan
C1s	291.28	284.84	282.38	4569.24	1.46	4589.9	22.94	C1s
O1s	535.88	531.39	527.68	25389.11	1.69	25788.42	47.01	O1s
Ni3p	77.93	68.15	64.98	1902.97	2.51	2083.3	20.24	Ni-Fe
Fe3p	63.58	56.74	52.68	423.4	3.09	507.34	6.53	Ni-Fe
S2p	170.68	168.18	166.28	307.81	2.19	373.86	3.27	S2p

Table S2 XPS patterns of the HT-LDH/CB product

Name	Start BE	Centre BE	End BE	Height CPS	FWHM eV	PP Height CPS	PP At. %	Title Scan
C1s	294.08	284.9	282.08	7528.99	1.39	8087.86	64.34	C1s
O1s	537.68	532.69	528.78	13581.58	2.18	13606.22	20.79	O1s
Ni3p	79.11	69.56	66.16	1112.42	2.93	1243.1	10.12	Ni-Fe
Fe3p	62.91	58.06	53.23	236.09	3.27	294.42	3.18	Ni-Fe
S2p	172.68	169.65	167.48	197.63	2.42	215.16	1.58	S2p

Notes and references

1. X. Wang, S. Zhou, W. Y. Xing, B. Yu, X. M. Feng, L. Song and Y. Hu, *J. Mater. Chem. A*, 2013, **1**, 4383-4390.
2. T. Iwasaki, H. Yoshii, H. Nakamura and S. Watano, *Appl. Clay Sci.*, 2012, **58**, 120-124.
3. L.-J. Zhou, X. Huang, H. Chen, P. Jin, G.-D. Li and X. Zou, *Dalton Transactions*, 2015, **44**, 11592-11600.
4. S. Z. Zhao, H. H. Yi, X. L. Tang, D. J. Kang, H. Y. Wang, K. Li and K. J. Duan, *Appl. Clay Sci.*, 2012, **56**, 84-89.